


SCIENTIFIC REPORTS



OPEN

Liraglutide improves liver microvascular dysfunction in cirrhosis: Evidence from translational studies

Fernanda Cristina de Mesquita^{1,3}, Sergi Guixé-Muntet^{1,2}, Anabel Fernández-Iglesias¹, Raquel Maeso-Díaz¹, Sergi Vila¹, Diana Hide¹, Martí Ortega-Ribera¹, José Luís Rosa⁴, Juan Carlos García-Pagán^{1,2}, Jaime Bosch^{1,2}, Jarbas Rodrigues de Oliveira³ & Jordi Gracia-Sancho¹ 

Hepatic stellate cells (HSC) play a key role in the development of chronic liver disease (CLD). Liraglutide, well-established in type 2 diabetes, showed anti-inflammatory and anti-oxidant properties. We evaluated the effects of liraglutide on HSC phenotype and hepatic microvascular function using diverse pre-clinical models of CLD. Human and rat HSC were *in vitro* treated with liraglutide, or vehicle, and their phenotype, viability and proliferation were evaluated. In addition, liraglutide or vehicle was administered to rats with CLD. Liver microvascular function, fibrosis, HSC phenotype and sinusoidal endothelial phenotype were determined. Additionally, the effects of liraglutide on HSC phenotype were analysed in human precision-cut liver slices. Liraglutide markedly improved HSC phenotype and diminished cell proliferation. Cirrhotic rats receiving liraglutide exhibited significantly improved liver microvascular function, as evidenced by lower portal pressure, improved intrahepatic vascular resistance, and marked ameliorations in fibrosis, HSC phenotype and endothelial function. The anti-fibrotic effects of liraglutide were confirmed in human liver tissue and, although requiring further investigation, its underlying molecular mechanisms suggested a GLP1-R-independent and NF- κ B-Sox9-dependent one. This study demonstrates for the first time that liraglutide improves the liver sinusoidal milieu in pre-clinical models of cirrhosis, encouraging its clinical evaluation in the treatment of chronic liver disease.

Glucagon-like peptide-1 (GLP-1) receptor agonists (GLP-1RA) are a new class of anti-diabetic medications that mimic the effects of incretin hormones¹. As an incretin hormone, which is synthesized in response to food intake, GLP-1 can stimulate insulin release by pancreatic β -cells in a glucose-dependent manner and suppress glucagon secretion from α -cells². The favourable actions of GLP-1 on glucose homeostasis are mediated through GLP-1 receptors. However, native GLP-1 is rapidly degraded in circulation³. Liraglutide, a synthetic GLP-1RA that shares 97% homology with the structure of human GLP-1, possesses a much longer circulating half-life, thereby making it a novel anti-diabetic drug suitable for once-daily injection¹. Apart from the pancreatic islets, GLP-1 receptors are present in many other tissues and, although its expression within the liver is not clear^{4,5}, recent studies demonstrated efficacy of GLP-1RA in liver diseases, such as NAFLD^{6,7}. In this regard, studies showed other beneficial properties for this type of drugs, including anti-inflammatory and anti-oxidant^{8,9}, which are also important for the resolution of chronic liver disease (CLD).

Cirrhosis is the end stage of CLD that starts with deregulations in the phenotype of all hepatic cells leading to parenchymal and sinusoidal dysfunction¹⁰. In CLD, both architectural alterations of the liver parenchyma and

¹Liver Vascular Biology Research Group, Barcelona Hepatic Hemodynamic Lab, IDIBAPS Biomedical Research Institute - CIBEREHD, Barcelona, Spain. ²University of Barcelona Medical School, Barcelona, Spain. ³Laboratório de Biofísica Celular e Inflamação, PUCRS, Porto Alegre, RS, Brazil. ⁴Departament de Ciències Fisiològiques, IDIBELL, Universitat de Barcelona, L'Hospitalet de Llobregat, Barcelona, Spain. Fernanda Cristina de Mesquita, Sergi Guixé-Muntet and Anabel Fernández-Iglesias contributed equally to this work. Jarbas Rodrigues de Oliveira and Jordi Gracia-Sancho jointly supervised this work. Correspondence and requests for materials should be addressed to J.G.-S. (email: jordi.gracia@idibaps.org)

sinusoidal microvascular dysfunction contribute to the development of portal hypertension¹¹. Architectural distortion of the cirrhotic liver is mainly due to excessive synthesis and deposition of extracellular matrix performed by deregulated fibrogenic cells mainly hepatic stellate cells (HSC)¹². Indeed, in response to liver injury, HSC gradually transdifferentiate to an activated α -SMA-positive phenotype with extensive proliferation, and high vasoconstrictive and pro-inflammatory properties^{13,14}. It is widely accepted that activation of HSC is a key factor in the pathogenesis of liver fibrosis, CLD and portal hypertension¹⁵. Moreover, an intimate crosstalk between HSC and other sinusoidal cells further contributes to the development and aggravation of CLD¹⁶.

CLD may improve in response to injury cessation, blockade of pro-fibrogenic mediators or drug-induced HSC inactivation¹⁷. Unfortunately, current treatment options for CLD and its main complication portal hypertension are limited, and importantly there is no effective therapy available to efficiently ameliorate the hepatic microcirculation of CLD¹⁸. Therefore, novel therapeutic strategies based on EMA/FDA approved drugs with no systemic adverse effects are required to improve treatments for patients with CLD.

The primary purpose of the present study was to evaluate the effects of liraglutide on HSC phenotype, liver microvascular function and underlying mechanisms in pre-clinical models of CLD.

Results

Liraglutide improves the phenotype of Hepatic Stellate Cells. Effects of liraglutide on HSC phenotype were assessed in diverse pre-clinical models of CLD. After preliminary dose- and time-response experiments (Supplementary Fig. 1), we characterized liraglutide's effects promoting the de-activation of cirrhotic primary hHSC and in the prevention of activation of control primary hHSC undergoing 7-day plastic activation. Both conditions showed a marked down-regulation in the activation markers collagen I and α -SMA at a concentration of 50 μ M and after 72 h of treatment (Fig. 1A left and middle panels). The anti-fibrotic effects of liraglutide were further validated in human precision-cut liver slices (PCLS) (Fig. 1A right). In addition, the amelioration in hHSC phenotype in response to liraglutide was validated using a functional assay. As shown in Fig. 1B, liraglutide significantly prevented the contraction of primary hHSC.

The effects of liraglutide on activated HSC were further analyzed in LX-2, a widely-accepted human cell line mimicking activated HSC. These experiments indeed showed de-activation of LX-2 cells in response to liraglutide (Fig. 2A), which was associated with significant reductions in the pro-inflammatory and pro-fibrogenic markers TNF- α and TGF- β 1 (Fig. 2A).

Interestingly, LX-2 cells treated with liraglutide showed no significant changes in viability when compared to controls, as observed with the double staining with AO-PI (Fig. 2B). Contrarily, using two different analysis of cell proliferation, the trypan blue exclusion assay and the expression of the proliferative marker PDGFR β , we herein show the anti-proliferative effects of liraglutide in HSC (Fig. 2C), which were accompanied with a marked reduction in their contraction ability (Fig. 2D). Altogether, validating the global improvement in HSC phenotype in response to liraglutide.

Similar beneficial effects of liraglutide were observed in rat primary HSC (Supplementary Fig. 2).

Liraglutide improves HSC phenotype and portal hypertension in CLD-rats. The potential beneficial effects of liraglutide as a new therapeutic strategy to improve CLD and portal hypertension were also analyzed *in vivo*. After 15 days of treatment, CLD-rats treated with liraglutide displayed lower expression of α -SMA and PDGFR β (Fig. 3A), accompanied by reductions in extracellular matrix synthesis and deposition as demonstrated by diminished collagen expression and hepatic fibrosis (Fig. 3B). No significant differences in TIMPs and MMPs were observed, thus suggesting that the peak of fibrinolysis already occurred (Supplementary Fig. 3). No effects on HSC viability (desmin expression) were observed, thus supporting the results obtained *in vitro*. Additional analysis of HSC phenotype in cells freshly isolated from CLD-rats treated with liraglutide, or vehicle, confirmed the marked beneficial effects of the drug promoting HSC deactivation (Fig. 3C).

Possible beneficial effects of liraglutide on hepatic and systemic hemodynamics in CLD-rats were also analyzed. Table 1 shows the morphometric and hemodynamic data from these animals. As expected, CLD-rats treated with liraglutide exhibited a slight but significant reduction in body weight, which is in agreement with previous studies¹⁹. Importantly, liraglutide-treated animals showed significantly lower portal pressure than vehicle-treated animals (11.6 ± 0.8 vs. 9.3 ± 1.0 mmHg; -20% ; $p = 0.03$) without changes in portal blood flow, thus suggesting an improvement in the hepatic vascular resistance (9.5 ± 1.8 vs. 5.7 ± 1.3 mmHg·mL·min⁻¹·g⁻¹; -23% ; $p = 0.1$). No effects of liraglutide on systemic hemodynamic or biochemical tests were observed.

Intrahepatic microcirculatory amelioration in response to liraglutide was further confirmed analyzing the hepatic microvascular phenotype. Indeed, LSEC from animals receiving liraglutide showed a significant reversal in their capillarization, as suggested by marked increments in fenestrae frequency and porosity (Fig. 4A), and a trend to higher nitric oxide bioavailability (Fig. 4B). In addition, characterization of the hepatic microvascular function *ex vivo* confirmed the global sinusoidal improvement, as demonstrated by reduction in HVR (Table 1) and improved liver vascular response to incremental doses of acetylcholine (Fig. 4C).

Liraglutide has a complementary effect with simvastatin improving HSC. Treatment of LX-2 cells with liraglutide did not modify the expression of the simvastatin-inducible transcription factor KLF2 (Supplementary Fig. 4 left). However, LX-2 treated with liraglutide or simvastatin showed reduced levels of α -SMA in the same magnitude. Interestingly, when both drugs were combined further reduced α -SMA (Supplementary Fig. 4 right), altogether suggesting that liraglutide has a complementary effect to simvastatin improving the phenotype of activated HSC.

Liraglutide improves HSC phenotype and liver microcirculation probably through a GLP1-R independent mechanism. Analysis of GLP1-R expression in rat and human liver tissues and HSC showed

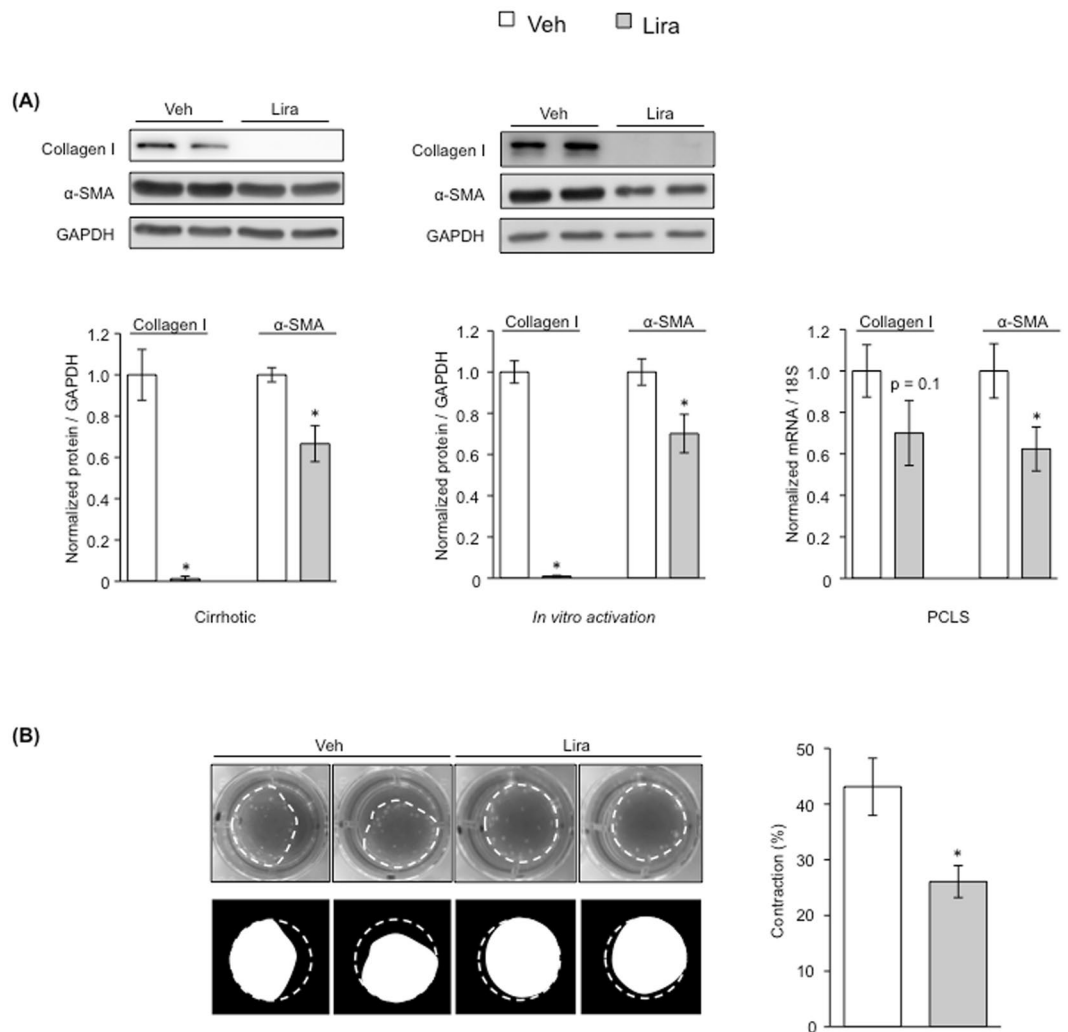


Figure 1. Amelioration of human primary HSC in response to liraglutide. **(A)** Expression of depicted proteins/genes after *in vitro* treatment with 50 μM liraglutide or vehicle in: 1-HSC isolated from cirrhotic human livers (left), 2-quiescent human HSC undergoing *in vitro* activation (middle), and 3-human precision-cut liver slices (PCLS) (right). **(B)** Effects of liraglutide, or its vehicle, on the contraction of primary human HSC. n = 3 per experimental condition. *p < 0.05 vs. vehicle.

no detectable mRNA expression (Supplementary Fig. 5A), while a band corresponding to 53 kDa (predicted GLP-1R molecular weight) was only detected in LX-2 and barely present in cirrhotic and NASH human livers, but not in control human or rat livers (either control or cirrhotic) (Supplementary Fig. 5B). Accordingly, analysis of the GLP-1R secondary messenger PKA in rHSC and LX-2 treated with liraglutide did not show differences in its phosphorylation in comparison to cells treated with vehicle (Supplementary Fig. 5C), and incubation of LX-2 with the GLP-1R antagonist Exendin 9–39 did not affect the de-activation effects of liraglutide (Supplementary Fig. 5D). Oppositely, liraglutide did repress the NF-κB molecular pathway (Supplementary Fig. 6).

Discussion

The major findings of the current study are that liraglutide promotes a marked amelioration in the phenotype of activated HSC, which in a pre-clinical model of chronic liver disease leads to significant improvement in portal hypertension and liver fibrosis. Importantly, the de-activating effects of liraglutide are herein demonstrated in human primary HSC and human liver tissue.

Liraglutide was developed as an anti-diabetic drug predictably acting on GLP-1R in pancreatic β-cells. Interestingly, different studies have demonstrated that these receptors may not be only limited to pancreatic β-cells. Considering the beneficial anti-inflammatory effects of GLP-1R agonists on cardiac fibrosis and NASH^{20–22}, we aimed the present study at analyzing the effects of liraglutide in chronic liver disease (CLD).

Liver cirrhosis is the end stage situation of CLD being the main triggering factor a complex multicellular response of all hepatic cells. Indeed, in front of a chronic injury both parenchymal and non-parenchymal cells undergo profound changes in their phenotype, becoming highly de-regulated and ultimately leading to fibrosis and microvascular dysfunction¹⁶. The most relevant clinical consequence of sinusoidal cells de-regulation is the

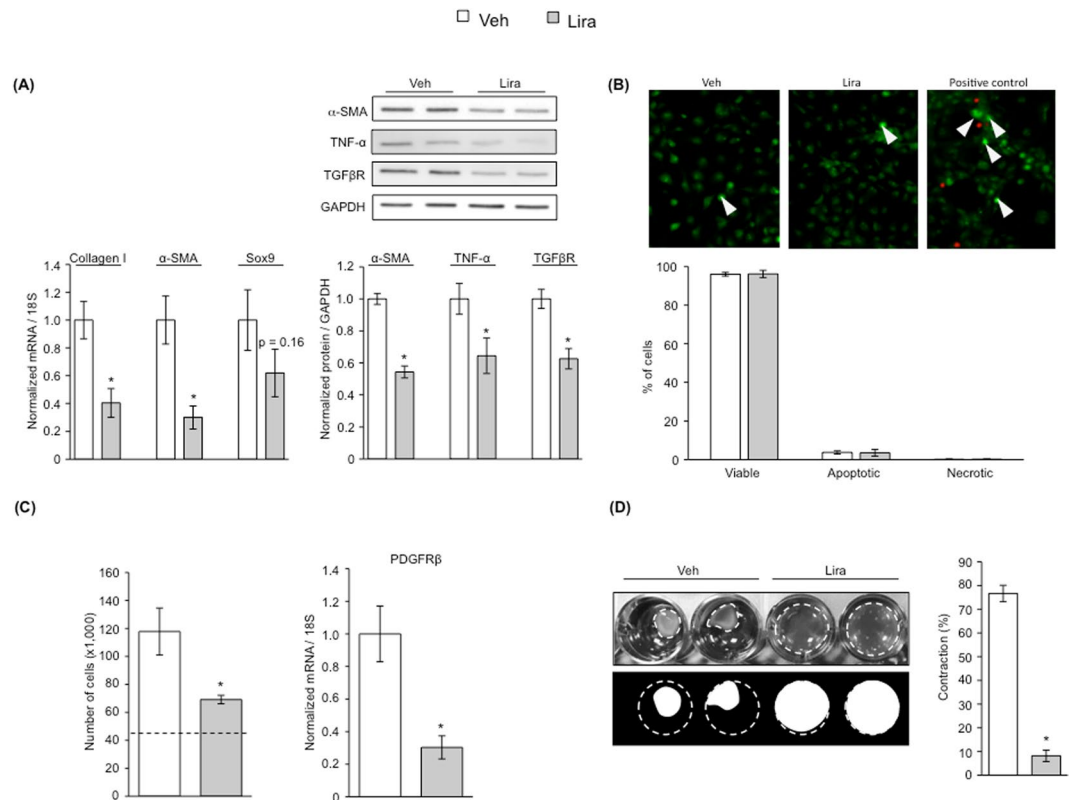


Figure 2. Underlying effects of HSC deactivation due to liraglutide. After 72 h of treatment with 50 μ M liraglutide, LX-2 cells were assessed for markers of HSC activation (A), cell viability by double staining with acridine orange (green dense nuclei: apoptosis, indicated by arrowheads) and propidium iodide (red cells: necrosis) (B), HSC proliferation assessed by cell counting and expression of the proliferative marker PDGFR β (C), and cell contraction (D). n = 3 per experimental condition. *p < 0.05 vs. vehicle.

development of portal hypertension, which derives both from pathological increases in intrahepatic vascular resistance and in portal blood flow. Considering the importance of HSC in CLD progression and aggravation, many studies focused on liver-specific drugs capable of inactivating the HSC, however few studies have advanced to the clinical stage²³.

Our study is the first showing that liraglutide is able to improve the phenotype of HSC. Indeed, we performed dose- and time-dependent experiments indicating that liraglutide de-activates HSC as demonstrated by reduced expression of α -SMA and collagen. Similarly, we observed prevention of HSC activation in response to liraglutide, therefore suggesting possible beneficial effects of the drug when administered at early stages of CLD. Importantly, we planned this study as a bed to bench-side one, and not vice versa, therefore firstly evaluating the effects of liraglutide in human primary HSC, to latterly use different preclinical models of CLD to further study the molecular mechanisms of such ameliorations.

Hepatic stellate cells are activated in response to different liver injuries, or due to paracrine factors, promoting tissue repair. Their response includes cell mobilization, proliferation, migration towards the lesion, and production of extracellular matrix components. When continuous liver injury occurs, HSC become chronically activated, acquire high expression of pro-inflammatory, pro-fibrogenic and proliferative markers like TNF- α , TGF β and PDGFR β , ultimately representing the main cell-type responsible for fibrosis deposition^{24, 25}. In the present study, we show that improvement in HSC phenotype in response to liraglutide was accompanied by marked reductions in the expression of these cytokines and proliferation markers, without affecting cell viability. Altogether suggesting that liraglutide promotes the de-activation of HSC, reduces their proliferation but does not induce cell apoptosis. Such anti-inflammatory effects, which are potentially optimal for the resolution of liver fibrosis *in vivo*, are quite different from previous studies showing concomitant de-activation and apoptosis/necrosis of HSC in response to certain therapeutic strategies^{26–28}. Importantly, analysis of HSC was not limited to molecular markers, but also included the cell contraction functional assay, which further confirmed the global improvement of HSC phenotype in response to liraglutide.

Additionally, we tested the possible beneficial effects of liraglutide when administered to human liver tissue. Taking advantage of the precision cut liver slices technique, considered an excellent tool to analyze the effects of drugs within the liver²⁹, we observed marked reductions in the expression of α -SMA and collagen in response to liraglutide, therefore corroborating the anti-fibrotic effects of the drug.

Once the phenotype of HSC was characterized *in vitro*, we studied the effects of a physiological-relevant dose of liraglutide administered *in vivo*. Liraglutide treatment markedly improved both HSC and LSEC phenotypes.

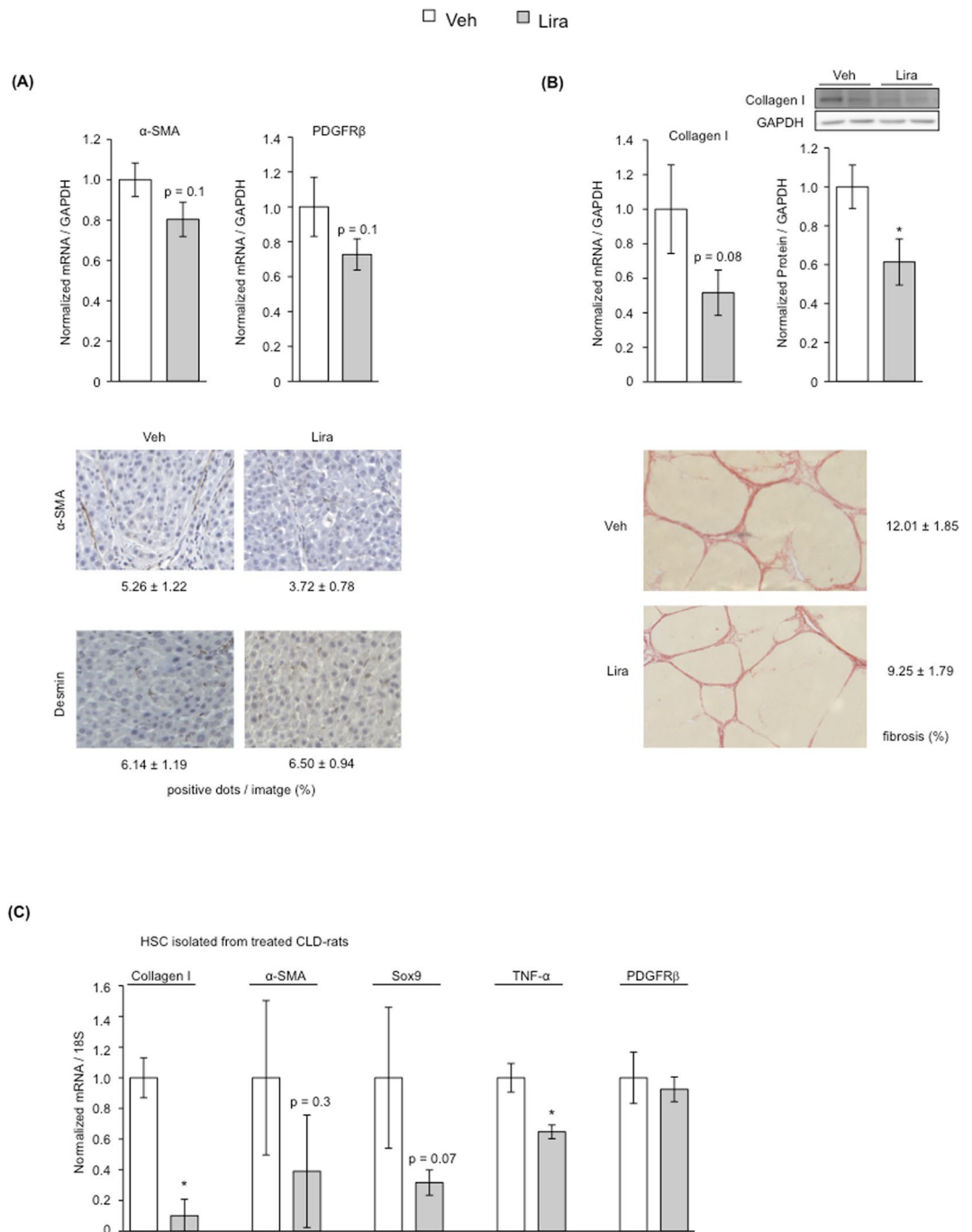


Figure 3. Analysis of HSC phenotype and liver fibrosis in CLD-rats treated with liraglutide. **(A)** Expression of HSC activation markers (α -SMA and PDGFR β) and Desmin in livers from TAA-CLD-rats treated for 15 days with liraglutide or vehicle. **(B)** Analysis of hepatic fibrosis in rats described in A (collagen I expression and Sirius Red staining). **(C)** Analysis of the phenotype of HSC freshly isolated from rats described in **(A)**. * $p < 0.05$ vs. vehicle. $n = 8$ (**A** and **B**) and $n = 3$ (**C**) per group. Results are indicated as mean \pm s.e.m.

In fact, HSC activation markers collagen I, α -SMA and PDGFR β were reduced in CLD rats receiving liraglutide, which was accompanied by amelioration in LSEC fenestrae and NO bioavailability. Although we herein demonstrate direct action of liraglutide on HSC, we do not rule out possible paracrine interactions between both sinusoidal cell types in response to the drug^{16,30}. Importantly, global improvement in the sinusoidal phenotype led to regression of liver fibrosis, and to significant amelioration in the hepatic microvascular dysfunction. Indeed, liraglutide was able to reduce the PP in rats with CLD and portal hypertension. Such improvement in hepatic hemodynamics was mostly due to a significant improvement in the intrahepatic microvascular dysfunction, as demonstrated by the estimations of the *in vivo* and *ex vivo* HVR, and the analysis of the *ex vivo*

	Vehicle n = 11	Liraglutide n = 11	p value
PP (mmHg)	11.6 ± 0.8	9.3 ± 1.0	0.03
MAP (mmHg)	99.5 ± 7.2	89.9 ± 7.1	0.4
PBF (mL/min)	11.9 ± 1.0	11.5 ± 2.3	0.5
HVR (mmHg·min·mL ⁻¹ ·g ⁻¹)	9.5 ± 1.8	5.7 ± 1.3	0.1
<i>ex vivo</i> HVR (mmHg·min·mL ⁻¹ ·g ⁻¹)	1.6 ± 0.3	0.9 ± 0.04	0.07
Body weight pre-treatment (g)	289 ± 12	288 ± 7	0.5
Body weight post-treatment (g)	310 ± 9	274 ± 9	0.03
Liver weight (g)	8.4 ± 0.7	6.7 ± 0.4	0.1
AST (U/L)	105 ± 14	126 ± 14	0.3
ALT (U/L)	61 ± 10	67 ± 4	0.5
Albumin (g/L)	15.3 ± 1.3	16.3 ± 0.5	0.5
Cholesterol (mg/dL)	54.0 ± 8.3	44.6 ± 5.8	0.4
TG (mg/dL)	31.2 ± 5.6	26.8 ± 3.4	0.5
FFA (μmol/L)	506 ± 66	477 ± 55	0.7

Table 1. Effects of Liraglutide on hepatic and systemic hemodynamics, and biochemical parameters in rats with chronic liver disease due to chronic TAA administration, represented as mean ± s.e.m. PP, portal pressure; MAP, mean arterial pressure; PBF, portal blood flow; HVR, hepatic vascular resistance; AST, aspartate aminotransferase; ALT, alanine aminotransferase; TG, triglycerides; FFA, free fatty acids.

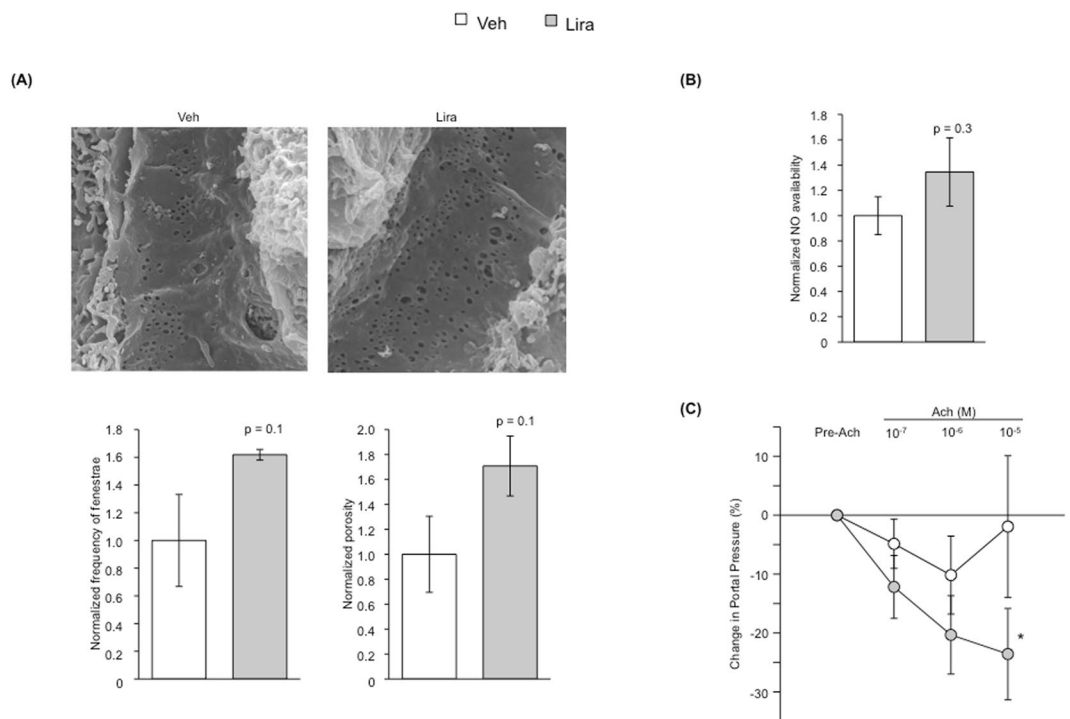


Figure 4. Effects of liraglutide on hepatic endothelial phenotype and microvascular function. **(A)** Liver sinusoidal fenestrae analysis by means of frequency (no. fenestrae/cell area) and porosity (fenestrae area/cell area) in TAA-CLD-rats treated with liraglutide or vehicle. **(B)** Hepatic nitric oxide (NO) bioavailability in rats described in A. **(C)** Hepatic microvascular function, calculated as the decrease in portal pressure in response to increasing doses of the endothelium-dependent vasodilator acetylcholine after vasoconstriction with methoxamine. * $p < 0.05$ vs. vehicle. $n = 3$ (A), $n = 8$ (B) and $n = 5$ (C) per group.

vasodilatory capacity in response to incremental doses of acetylcholine. Importantly, liraglutide did not affect systemic hemodynamics.

We next ascertained which could be the molecular pathway underlying liraglutide effects on HSC, and consequently on liver microcirculation and fibrosis. First, and considering that liraglutide was formulated to act on GLP-1 receptor, we analyzed the expression of this receptor both in HSC isolated from rat and humans, and also in liver tissues. Surprisingly, GLP-1R mRNA was not detected in whole liver homogenates, primary human HSC

or LX-2 cells using two different Taqman probes with PCR reactions going up to 60 cycles. At the protein level, western blot of hepatic samples using an antibody against GLP-1R showed signal in LX-2 lysates at the predicted GLP-1R molecular weight, but this signal was barely present in cirrhotic and NASH human tissue, while it was not detected in control human livers or rat liver tissue (either control or cirrhotic). These observations suggest that the beneficial effects of liraglutide in rat HSC and its effects *in vivo* would not be dependent on GLP-1R. Previous reports already showed contradictory results in terms of GLP-1R expression within the liver^{4,5}, and we are not totally convinced that the band detected by the antibody in human samples really corresponds to GLP-1R (as it is contradictory to the two specific mRNA TaqMan probes). In agreement, additional experiments showed lack of protein kinase A phosphorylation (marker of GLP-1R activation)^{31,32} in response to liraglutide, and no differences in liraglutide-mediated HSC de-activation and proliferation when an antagonist of GLP-1R was used. Secondly, we analyzed the expression of the transcription factor Kruppel-like factor 2 (KLF2) in response to liraglutide since the effects of liraglutide on HSC were quite similar to those previously observed using statins^{26,33–35}. These experiments showed no up-regulation in response to the drug, moreover a synergistic effect of liraglutide and simvastatin de-activating HSC was observed, thus suggesting that they act by different pathways and could be used in combination at the bedside. Lastly, we evaluated the NF- κ B molecular pathway, which plays a major role in liver fibrosis³⁶ and is inhibited by liraglutide in the endothelium³⁷. Interestingly, liraglutide down-regulated the expression of NF- κ B, and also of its target gene Sox9.

With these results we cannot delineate the exact molecular mechanism driving liraglutide's beneficial effects, which represents a limitation of the study. Nevertheless, considering the main role of NF- κ B and Sox9 modulating HSC phenotype^{38,39}, and the findings described above, we herein suggest that in the specific scenario of CLD liraglutide may improve HSC phenotype and liver microcirculation through a GLP-1R independent mechanism, being the NF- κ B–Sox9 pathway a solid candidate to mediate, at least in part, these effects. Desirable future experiments, out of the scope of the present study, will clarify the specific receptor and the molecular mechanisms that mediate the beneficial effects of this drug in chronic liver disease.

In conclusion, the present study describes the anti-fibrotic effects of liraglutide both in rodent and, importantly, human pre-clinical models of chronic liver disease, therefore encouraging its application at the bedside as new therapeutic tool to improve cirrhosis and portal hypertension. Moreover, the potential results of the LEAN trial opens the possibility to use liraglutide not only to improve mild NASH⁷, but promote regression of advanced chronic liver disease. Desirable future trials will clarify this promising therapeutic alternative.

Materials and Methods

Animal models of chronic liver disease (CLD). The study was carried out in male Wistar rats (Charles River Laboratories, Barcelona, Spain). Animals were kept in environmentally controlled animal facilities. All procedures were approved by the Laboratory Animal Care and Use Committee of the University of Barcelona and were conducted in accordance with the European Community guidelines for the protection of animals used for experimental and other scientific purposes (EEC Directive 86/609). The personnel who prepared and administered treatments and those that performed the experimental studies were different. Treatment's codes were not open for interpretation of the results until the inclusion of all animals.

Induction of CLD by thioacetamide (TAA). TAA (Sigma Chemical Co) was dissolved in 0.9% normal saline approximately one hour before injection. Treatment groups received 200 mg/kg of TAA twice per week for a total of 12 weeks while control groups received the same volume of 0.9% normal saline¹⁸.

Induction of CLD by Carbon Tetrachloride (CCl₄). Rats underwent inhalation exposure to CCl₄ (Sigma) and received phenobarbital (0.3 g/L) in the drinking water. When rats developed ascites, toxicants administration was stopped⁴⁰.

HSC isolation, culture and treatments. *Isolation and culture of HSC.* HSC were isolated from human (hHSC: control or cirrhotic) and rat (rHSC: control, TAA-CLD or CCl₄-CLD) livers as described²⁶ with minor modifications. Briefly, liver tissues were perfused with collagenase A, pronase and DNase (all Roche) in Gey's Balanced Salt Solution (GBSS; Sigma), and dispersed cells were fractionated by density gradient centrifugation using 11.5% Optiprep (Sigma). HSC were cultured in Iscove's Modified Dulbecco's Media (IMDM, Invitrogen, Gibco) supplemented with fetal bovine serum, glutamine, antibiotics and amphotericin B. Results using primary HSC derived from at least 3 independent isolations and 3 replicates.

Immortalized human-activated HSC LX-2 were cultured as described¹¹. Results using LX-2 derived from at least three replicates per experimental condition.

HSC treatments. HSC were incubated with liraglutide (Novo Nordisk), or its vehicle PBS, at different concentrations (1 μ M, 10 μ M, 50 μ M and 100 μ M) and for different periods of time (24 h, 48 h and 72 h). *In vitro* dosing of liraglutide was based on previous literature⁴¹. Considering that liraglutide exerted beneficial effects at 50 μ M and after 72 h of treatment, all subsequent experiments were performed using these experimental conditions. Simvastatin was used in 10 μ M dose alone and in combination with liraglutide. Exendin fragment 9–39 (Sigma-Aldrich; 10 nM–1 μ M) was used as a GLP-1R antagonist⁴¹.

Cell viability and proliferation. Equal number of LX-2 were seeded and after 72 h of liraglutide or vehicle, floating and adhered cells were collected and counted using a hemocytometer with trypan blue dye exclusion (FLUKA).

Cell apoptosis. Cells were incubated with fresh medium containing 800 ng/mL Acridine Orange (AO) and 5 µg/mL Propidium Iodide (PI) for 10 min at 37 °C and then washed with PBS. Fresh medium was added and cell death was examined using a fluorescence microscope (Olympus BX51, Tokyo, Japan) equipped with a digital camera (Olympus, DP72). AO is a metachromatic dye that stains both viable and apoptotic cells by intercalating into DNA and emits green fluorescence upon excitation at 480–490 nm. Nevertheless, nuclear condensation that occurs during apoptosis glares a more intense fluorescence. PI is excluded by viable cells but can penetrate cell membranes of dying or dead cells due to necrosis, emitting red fluorescence. Positive controls (*in vitro* ischemia and reperfusion), and negative controls (without dye) were included²⁶.

Cell contraction. Contraction of HSC was performed as previously described with some modifications⁴². Briefly, culture plates were incubated with 1% BSA-PBS and afterwards filled with a mix of collagen (2 mg/mL) and human HSC (1–2 × 10⁵ cells/mL). Once the gels were solidified, serum free IMDM with 50 µM liraglutide or vehicle was added. After 24 h, contraction was induced by adding 10% FBS for 24 h. Finally, the contraction area was digitalized and measured with ImageJ software. The results are expressed as % of contraction relative to the initial area of the gel.

Characterization of CLD-rats treated with liraglutide. *Liraglutide administration.* TAA-CLD-rats received by subcutaneous injections, twice a day, either liraglutide (0.5 mg/kg/day; n = 11) or vehicle (0.9% NaCl; n = 11) during 15 days. The dose was selected based on a conversion calculation starting from the dose used in humans and agreed with previous publications^{19,43,44}. Administration of liraglutide to CLD-rats started one week after stopping the administration of TAA.

In vivo hemodynamics. Rats (n = 8 per group) were anesthetized with ketamine hydrochloride (100 mg/Kg; Merial Laboratories) plus midazolam (5 mg/kg; Laboratorios Reig Jofré) intraperitoneally. A tracheotomy was performed and a polyethylene tube PE-240 was inserted into the trachea to ensure a patent airway. PE-50 catheters were introduced into the femoral artery to measure mean arterial pressure (MAP; mmHg) and into ileocolic vein to measure portal pressure (PP; mmHg). A perivascular ultrasonic flow probe (Transonic System) was placed around the portal vein, as close as possible to the liver to avoid portal-collateral blood flow, in order to measure portal blood flow (PBF; mL·min⁻¹). Hepatic vascular resistance (mmHg·min·mL⁻¹·g⁻¹) was calculated as: PP/PBF. Blood pressures and flows were registered on a multichannel computer based recorder (Power Lab; AD Instruments). Temperature of the animals was maintained at 37 ± 0.5 °C and hemodynamic data were collected after 20 min stabilization^{40,45}. Blood serum and plasma samples were stored for biochemical analysis.

Liver microvascular function. Immediately after recording *in vivo* hemodynamics, rat livers were isolated and perfused with Krebs buffer as previously described (n = 5 per group)^{45,46}. The perfused rat liver preparation was allowed to stabilize for 20 min before vasoactive substances were added. Intrahepatic microcirculation was pre-constricted by adding the α1-adrenergic agonist methoxamine (Mtx; 10⁻⁴ M; Sigma) to the reservoir, and liver microvascular function was assessed as concentration–response curves to cumulative doses of acetylcholine (Ach; 10⁻⁷–10⁻⁵ M; Sigma). Liver tissue was snap-frozen for subsequent molecular analysis.

Evaluation of hepatic fibrosis. CLD-rat livers were fixed in 10% formalin, embedded in paraffin, sectioned, and stained with 0.1% Sirius Red, photographed, and analyzed using a microscope equipped with a digital camera. The red-stained area was measured using Axiovision software²⁶. Values are expressed as the mean of 8 fields per sample.

Sinusoidal characterization using Scanning Electron Microscope. In a sub-group of animals (n = 3 per group), after obtaining *in vivo* hemodynamics, livers were perfused through portal vein with a solution containing 2.5% glutaraldehyde and 2% paraformaldehyde and fixed overnight at 4 °C. Samples were washed 3 times with 0.1 M cacodylate buffer. Liver sections were fixed with 1% osmium in cacodylate buffer, dehydrated in ethanol, and dried with hexamethyldisilazane. Six randomly selected blocks from each animal were mounted onto stubs, and sputter coated with gold. 10 images per animal were acquired at a resolution of 15,000x using a Jeol 6380 Scanning Electron Microscope (JEOL Ltd, Tokyo, Japan). Liver sinusoidal fenestrations were quantified using ImageJ Software (NIH)⁴⁷.

Nitric Oxide bioavailability. Levels of cGMP, a marker of NO bioavailability, were analyzed in liver homogenates using an enzyme immunoassay (Cayman Chemical Co., Ann Arbor, MI) as previously described⁴⁸.

RNA isolation and quantitative PCR. RNA from cells and tissue were extracted using RNeasy mini kit (Qiagen) and Trizol (Life Technologies), respectively. RNA quantification was performed using a NanoDrop spectrophotometer. cDNA was obtained using QuantiTect reverse transcription kit (Qiagen). Real-Time PCR were performed in an ABI PRISM 7900HT Fast Real-Time PCR System, using TaqMan predesigned probes for Col1A1 (Hs00164004_m1, Rn01463848_m1), α-SMA (Hs00426835_g1, Rn01759928_g1), PDGFRβ (Hs01019589_m1, Rn01491838_m1), GLP1-R (Hs00157705_m1, Hs01006326_m1), Sox9 (Hs00165814_m1, Rn01751070_m1) and GAPDH or 18S as endogenous controls. Results, expressed as 2^{-ΔΔCt}, represent the x-fold increase of gene expression compared with the corresponding control group.

Western blot analysis. Cells were rinsed twice with PBS and lysed with Triton lysis buffer. Livers were homogenized in triton-lysis buffer for whole protein extraction. Aliquots from each sample containing equal amounts of protein were run on a sodium dodecylsulphate polyacrylamide gel, and transferred to a nitrocellulose membrane. After the transfer, blots were blocked with Tris buffered saline containing 0.05% Tween-20 and 5% non-fat dry milk or 3% albumin and subsequently incubated overnight at 4 °C with primary antibodies

against collagen I (ABT123, Millipore), α -SMA (A2547, Sigma), TNF- α (sc-1351, Santa Cruz Biotechnology), TGF β R (sc-398, Santa Cruz Biotechnology), GAPDH (sc-32233, Santa Cruz Biotechnology), p-PKA (4781, Cell Signaling), NF- κ B (6956, Cell Signaling) and I κ B (4812, Cell Signaling), all at 1:1000 dilution. Then membranes were incubated with the appropriate horseradish peroxidase-conjugated secondary antibody at room temperature. Protein expression was determined by densitometric analysis using the LAS4000 (GE Healthcare) and Image Studio Lite software (LI-COR). Quantitative densitometric values of all proteins were normalized to GAPDH.

Precision-cut liver slices of human livers (PCLS). Fresh human liver biopsies were used to obtain 250 μ m slices using a Vibratome VT1000S (Leica Microsystems, Wetzlar, Germany). Samples were washed in PBS, soaked in 4% agarose solution (Ultrapure LMP Agarose, Invitrogen, Carlsbad, California, USA) for 20 min, and then orientated, mounted and immobilized using cyanoacrylate glue. Tissue slices were placed on organotypic tissue culture plate inserts (Millicell[®]-CM; Millipore). Tissues were maintained at 37 °C in a 5% CO₂ humidified incubator using 1.1 mL of Williams' Medium E supplemented with 1% inactivated fetal bovine serum, 2 mM L-Glutamine, 50 U/mL penicillin and 50 μ g/mL streptomycin. Tissue slices were incubated with 50 μ M liraglutide for 24 h. Sections were then transferred to a 1.5 mL tube and lysed for RNA isolation and qPCR²⁹.

Ethics information. Quiescent hHSC (for prevention of *in vitro* activation) and PCLS were obtained from remnants from partial hepatectomy. Livers were considered control, but exhibited fibrosis staging between F1 and F2. In all cases surgery was recommended to excise tumor metastasis from colon carcinoma. Cirrhotic hHSC (for *in vitro* de-activation) were isolated from remnant cirrhotic livers (all alcoholic aetiology) obtained after transplantation. The Ethics Committee of the Hospital Clinic de Barcelona approved the experimental protocol, samples manipulation and isolation procedures were carried out following good laboratory practices; in all cases patients signed the informed consent.

Statistical analysis. Statistical analysis was performed with the SPSS V.23.0 for Windows statistical package (IBM, Armonk, New York, USA). Results are expressed as mean \pm s.e.m. Normality of samples was assessed using the Kolmogorov Smirnov test. For samples following a normal distribution, comparisons between groups were performed with the Student t test or analysis of variance, followed by a Bonferroni Post Hoc test when adequate. Otherwise, comparisons were assessed with the non-parametric Mann-Whitney U or Kruskal Wallis test when adequate. Differences were considered significant at a *p* value < 0.05.

References

- Nauck, M. A. Incretin-based therapies for type 2 diabetes mellitus: properties, functions, and clinical implications. *Am. J. Med.* **124**, S3–18 (2011).
- Kazafeos, K. Incretin effect: GLP-1, GIP, DPP4. *Diabetes Res. Clin. Pract.* **93**(Suppl 1), S32–6 (2011).
- Drucker, D. J. The biology of incretin hormones. *Cell Death Differ.* **3**, 153–165 (2006).
- Gupta, N. A. *et al.* Glucagon-like peptide-1 receptor is present on human hepatocytes and has a direct role in decreasing hepatic steatosis *in vitro* by modulating elements of the insulin signaling pathway. *Hepatology* **51**, 1584–1592 (2010).
- Pyke, C. *et al.* GLP-1 Receptor Localization in Monkey and Human Tissue: Novel Distribution Revealed With Extensively Validated Monoclonal Antibody. *Endocrinology* **155**, 1280–1290 (2014).
- Wang, X.-C., Gusdon, A. M., Liu, H. & Qu, S. Effects of glucagon-like peptide-1 receptor agonists on non-alcoholic fatty liver disease and inflammation. *World J. Gastroenterol.* **20**, 14821–14830 (2014).
- Armstrong, M. J. *et al.* Liraglutide safety and efficacy in patients with non-alcoholic steatohepatitis (LEAN): a multicentre, double-blind, randomised, placebo-controlled phase 2 study. *Lancet (London, England)* **387**, 679–90 (2016).
- McClellan, P. L., Jalewa, J. & Hölscher, C. Prophylactic liraglutide treatment prevents amyloid plaque deposition, chronic inflammation and memory impairment in APP/PS1 mice. *Behav. Brain Res.* **293**, 96–106 (2015).
- Shiraki, A. *et al.* The glucagon-like peptide 1 analog liraglutide reduces TNF- α -induced oxidative stress and inflammation in endothelial cells. *Atherosclerosis* **221**, 375–82 (2012).
- Fernández-Iglesias, A. & Gracia-Sancho, J. How to face chronic liver disease: the sinusoidal perspective. *Front. Med.* **4**, 7 (2017).
- Marrone, G. *et al.* The transcription factor KLF2 mediates hepatic endothelial protection and paracrine endothelial-stellate cell deactivation induced by statins. *J. Hepatol.* **58**, 98–103 (2013).
- Pinzani, M. & Gentilini, P. Biology of hepatic stellate cells and their possible relevance in the pathogenesis of portal hypertension in cirrhosis. *Semin. Liver Dis.* **19**, 397–410 (1999).
- Török, N. J. Recent advances in the pathogenesis and diagnosis of liver fibrosis. *J. Gastroenterol.* **43**, 315–21 (2008).
- Soon, R. K. & Yee, H. F. Stellate Cell Contraction: Role, Regulation, and Potential Therapeutic Target. *Clin. Liver Dis.* **12**, 791–803 (2008).
- Reynaert, H. Hepatic stellate cells: role in microcirculation and pathophysiology of portal hypertension. *Gut* **50**, 571–581 (2002).
- Marrone, G., Shah, V. H. & Gracia-Sancho, J. Sinusoidal communication in liver fibrosis and regeneration. *J. Hepatol.* **65**, 608–17 (2016).
- Kisseleva, T. *et al.* Myofibroblasts revert to an inactive phenotype during regression of liver fibrosis. *Proc. Natl. Acad. Sci. USA* **109**, 9448–9453 (2012).
- Cerini, F. *et al.* Enoxaparin reduces hepatic vascular resistance and portal pressure in cirrhotic rats. *J. Hepatol.* **64**, 834–42 (2016).
- Gao, H. *et al.* The Glucagon-Like Peptide-1 Analogue Liraglutide Inhibits Oxidative Stress and Inflammatory Response in the Liver of Rats with Diet-Induced Non-alcoholic Fatty Liver Disease. *Biol. Pharm. Bull.* **694**, 694–702 (2015).
- Gaspari, T. *et al.* Molecular and cellular mechanisms of glucagon-like peptide-1 receptor agonist-mediated attenuation of cardiac fibrosis. *Diabetes Vasc. Dis. Res.* **13**, 56–68 (2016).
- Armstrong, M. J. *et al.* Glucagon-like peptide 1 decreases lipotoxicity in non-alcoholic steatohepatitis. *J. Hepatol.* **64**, 399–408 (2016).
- Steven, S. *et al.* Gliptin and GLP-1 analog treatment improves survival and vascular inflammation/dysfunction in animals with lipopolysaccharide-induced endotoxemia. *Basic Res. Cardiol.* **110**, 6 (2015).
- Schuppan, D. & Kim, Y. O. Evolving therapies for liver fibrosis. *J. Clin. Invest.* **123**, 1887–1901 (2013).
- Weiskirchen, R. & Tacke, F. Cellular and molecular functions of hepatic stellate cells in inflammatory responses and liver immunology. *Hepatobiliary Surg Nutr* **3**, 344–363 (2014).
- Trautwein, C., Friedman, S. L., Schuppan, D. & Pinzani, M. Hepatic fibrosis: Concept to treatment. *J. Hepatol.* **62**, S15–S24 (2015).
- Marrone, G. *et al.* KLF2 exerts antifibrotic and vasoprotective effects in cirrhotic rat livers: behind the molecular mechanisms of statins. *Gut* **64**, 1434–43 (2015).
- Klein, S. *et al.* Atorvastatin inhibits proliferation and apoptosis, but induces senescence in hepatic myofibroblasts and thereby attenuates hepatic fibrosis in rats. *Lab. Invest.* **92**, 1440–1450 (2012).

28. Wright, M. C. *et al.* Gliotoxin Stimulates the Apoptosis of Human and Rat Hepatic Stellate Cells and Enhances the Resolution of Liver Fibrosis in Rats. *Gastroenterology* **121**, 685–698 (2001).
29. Olinga, P. & Schuppan, D. Precision-cut liver slices: A tool to model the liver *ex vivo*. *J. Hepatol.* **58**, 1252–1253 (2013).
30. Xie, G. *et al.* Role of Differentiation of Liver Sinusoidal Endothelial Cells in Progression and Regression of Hepatic Fibrosis in Rats. *Gastroenterology* **142**, 918–927 (2012).
31. Laviola, L. *et al.* Glucagon-like peptide-1 counteracts oxidative stress-dependent apoptosis of human cardiac progenitor cells by inhibiting the activation of the c-Jun N-terminal protein kinase signaling pathway. *Endocrinology* **153**, 5770–81 (2012).
32. Wang, L. *et al.* GLP-1 analog liraglutide enhances proinsulin processing in pancreatic β -cells via a PKA-dependent pathway. *Endocrinology* **155**, 3817–28 (2014).
33. Abraldes, J. G. *et al.* Simvastatin treatment improves liver sinusoidal endothelial dysfunction in CCl₄ cirrhotic rats. *J. Hepatol.* **46**, 1040–6 (2007).
34. Trebicka, J. *et al.* Atorvastatin lowers portal pressure in cirrhotic rats by inhibition of RhoA/Rho-kinase and activation of endothelial nitric oxide synthase. *Hepatology* **46**, 242–253 (2007).
35. La Mura, V. *et al.* Effects of simvastatin administration on rodents with lipopolysaccharide-induced liver microvascular dysfunction. *Hepatology* **57**, 1172–1181 (2013).
36. Luedde, T. & Schwabe, R. F. NF- κ B in the liver—linking injury, fibrosis and hepatocellular carcinoma. *Nat. Rev. Gastroenterol. Hepatol.* **8**, 108–118 (2011).
37. Gaspari, T. *et al.* A GLP-1 receptor agonist liraglutide inhibits endothelial cell dysfunction and vascular adhesion molecule expression in an ApoE^{-/-} mouse model. *Diabetes Vasc. Dis. Res.* **8**, 117–24 (2011).
38. Pritchett, J. *et al.* Osteopontin is a novel downstream target of SOX9 with diagnostic implications for progression of liver fibrosis in humans. *Hepatology* **56**, 1108–1116 (2012).
39. Martin, K. *et al.* PAK proteins and YAP-1 signalling downstream of integrin beta-1 in myofibroblasts promote liver fibrosis. *Nat. Commun.* **7**, 12502 (2016).
40. Gracia-Sancho, J. *et al.* Endothelial expression of transcription factor Kruppel-like factor 2 and its vasoprotective target genes in the normal and cirrhotic rat liver. *Gut* **60**, 517–24 (2011).
41. Cantini, G. *et al.* Effect of liraglutide on proliferation and differentiation of human adipose stem cells. *Mol. Cell. Endocrinol.* **402**, 43–50 (2015).
42. Perri, R. E. *et al.* Defects in cGMP-PKG pathway contribute to impaired NO-dependent responses in hepatic stellate cells upon activation. *Am. J. Physiol. Gastrointest. Liver Physiol.* **290**, G535–42 (2006).
43. Lu, N. *et al.* Glucagon-like peptide-1 receptor agonist Liraglutide has anabolic bone effects in ovariectomized rats without diabetes. *PLoS One* **10**, e0132744 (2015).
44. Hoang, V., Bi, J., Mohankumar, S. M. & Vyas, A. K. Liraglutide Improves Hypertension and Metabolic Perturbation in a Rat Model of Polycystic Ovarian Syndrome. *PLoS One* **10**, e0126119 (2015).
45. Hide, D. *et al.* Effects of warm ischemia and reperfusion on the liver microcirculatory phenotype of rats: underlying mechanisms and pharmacological therapy. *Sci. Rep.* **6**, 22107 (2016).
46. Gracia-Sancho, J. *et al.* Evidence Against a Role for NADPH Oxidase Modulating Hepatic Vascular Tone in Cirrhosis. *Gastroenterology* **133**, 959–966 (2007).
47. Hilmer, S. N. *et al.* Age-related changes in the hepatic sinusoidal endothelium impede lipoprotein transfer in the rat. *Hepatology* **42**, 1349–1354 (2005).
48. Hide, D. *et al.* A novel form of the human manganese superoxide dismutase protects rat and human livers undergoing ischaemia and reperfusion injury. *Clin. Sci. (Lond)*. **127**, 527–37 (2014).

Acknowledgements

Authors are in debt with Drs Garcia-Valdecasas and Molina for providing human biopsies, Dr Bataller for providing LX-2 cells, and Bibiana Rius and Dr Clària for their expertise in PCLS. This work was funded by the Ministerio de Economía y Competitividad – Instituto de Salud Carlos III, FIS (PI14/00029 and PI13/00341), and the European Union (Fondos FEDER, “una manera de hacer Europa”). FcDm has a Fellowship from CAPES/Ciência sem Fronteiras - Brazil, and SG-M from the Fundació Catalana de Trasplantament. AF-I has a Sara Borrell contract from the Instituto de Salud Carlos III. CIBEREHD is funded by the Instituto de Salud Carlos III.

Author Contributions

F.C.dM., S.G.-M. and A.F.-I. designed the research, conceived ideas, performed experiments, and wrote the manuscript. R.M.-D., S.V., D. H. and M.O.-R. performed experiments and analyzed data. J.L.R. and J.C.G.-P. critically revised the manuscript. J.B. critically revised the manuscript and obtained funding. J.R.dO. conceived ideas and critically revised the manuscript. J.G.-S. designed the research, conceived ideas, wrote the manuscript, obtained funding and directed the study. All authors edited and reviewed the final manuscript.

Additional Information

Supplementary information accompanies this paper at doi:[10.1038/s41598-017-02866-y](https://doi.org/10.1038/s41598-017-02866-y)

Competing Interests: The authors declare that they have no competing interests.

Publisher's note: Springer Nature remains neutral with regard to jurisdictional claims in published maps and institutional affiliations.



Open Access This article is licensed under a Creative Commons Attribution 4.0 International License, which permits use, sharing, adaptation, distribution and reproduction in any medium or format, as long as you give appropriate credit to the original author(s) and the source, provide a link to the Creative Commons license, and indicate if changes were made. The images or other third party material in this article are included in the article's Creative Commons license, unless indicated otherwise in a credit line to the material. If material is not included in the article's Creative Commons license and your intended use is not permitted by statutory regulation or exceeds the permitted use, you will need to obtain permission directly from the copyright holder. To view a copy of this license, visit <http://creativecommons.org/licenses/by/4.0/>.

© The Author(s) 2017